

Optimal transport framework for efficient prototype selection

Karthik S. Gurumoorthy^{*†} Pratik Jawanpuria^{*‡} Bamdev Mishra^{*‡}

Abstract

Summarizing data via representative examples is an important problem in several machine learning applications where human understanding of the learning models and underlying data distribution is essential for decision making. In this work, we develop an optimal transport (OT) based framework to select informative prototypical examples that best represent a given target dataset. We model the prototype selection problem as learning a sparse (empirical) probability distribution having minimum OT distance from the target distribution. The learned probability measure supported on the chosen prototypes directly corresponds to their importance in representing and summarizing the target data. We show that our objective function enjoys a key property of submodularity and propose a parallelizable greedy method that is both computationally fast and possess deterministic approximation guarantees. Empirical results on several real world benchmarks illustrate the efficacy of our approach.

1 Introduction

Extracting informative and influential samples that best represent the underlying data-distribution is a fundamental problem in machine learning (Weiser, 1982; Bien & Tibshirani, 2011b; Kim et al., 2014; Koh & Liang, 2017; Yeh et al., 2018). As sizes of datasets have grown (accelerated by the advent of deep learning methods), summarizing a dataset with a collection of representative samples from it is of increasing importance to data scientists and domain-specialists (Bien & Tibshirani, 2011a). Prototypical samples offer interpretative value in every sphere of humans decision making where machine learning models have become integral such as healthcare (Caruana et al., 2015), information technology (Idé & Dhurandhar, 2017), and entertainment (Ribeiro et al., 2016), to name a few. In addition, extracting such compact synopses play a pivotal tool in depicting the scope of a dataset, in detecting outliers (Kim et al., 2016), and for compressing and manipulating data distributions (Rousseeuw & Kaufman, 2009). Existing works (Lozano et al., 2006; Wei et al., 2015) have also studied the generalization properties of machine learning models trained on a prototypical subset of large dataset. Hence, prototype selection also offer less resource-consuming alternatives to traditional large-scale training of machine learning models.

Works such as (Bien & Tibshirani, 2011b; Wei et al., 2015) consider selecting representative elements (henceforth also referred to as *prototypes*) in the supervised setting, i.e., the selection algorithm has access to the label information of the data points. Recent works (Kim et al., 2016; Gurumoorthy et al., 2019) have also explored the problem of prototype selection in the unsupervised setting, in which the selection algorithm has access only to the feature representation of the data points. They view the given dataset Y and a candidate prototype set P as empirical distributions q and p , respectively. Thus, the prototype selection problem is

^{*}Equal contribution.

[†]Amazon Development Center, India. gurumoor@amazon.com

[‡]Microsoft, India. Email: {pratik.jawanpuria,bamdevm}@microsoft.com.

modeled as searching for a distribution p (corresponding to a set P of data points, typically with a small cardinality) that is a good approximation of the distribution q . (Kim et al., 2016), for instance, proposed to employ the maximum mean discrepancy (MMD) distance (Gretton et al., 2006) to measure the similarity between the two distributions. While (Kim et al., 2016) assigns equal importance to the selected prototypical samples, (Gurumoorthy et al., 2019) builds on top of their framework to learn weights that correspond to the importance of each prototype.

In this paper, we focus on the unsupervised prototype selection and view it from the perspective of the optimal transport theory. The optimal transport (OT) framework provides a natural metric for comparing probability distributions while respecting the underlying geometry of the data (Villani, 2009; Peyré & Cuturi, 2019). Over the last few years, OT distances (also known as Wasserstein distances) have found widespread use in several machine learning applications such as image retrieval (Rubner et al., 2000), shape interpolation (Solomon et al., 2015), domain adaptation (Courty et al., 2017), supervised learning (Frogner et al., 2015), generative model training (Arjovsky et al., 2017), etc. The *transport plan*, learned while computing the OT distance between the source and target distributions, is the joint distribution between the source and the target distributions.

It should be noted that compared to MMD, the Wasserstein distance enjoys several advantages such as being faithful to the ground metric (i.e., geometry over the space of probability distributions) and identifying correspondences at the fine grained level of individual data points via the transport plan. On the other hand, as MMD induces the “flat” geometry of reproducing kernel Hilbert space (RKHS) on the the space of probability distributions as it measures the distance between the mean embeddings of distributions in the RKHS of a universal kernel (Smola et al., 2007; Gretton et al., 2006, 2012)). The individuality of data points is also lost while computing distance between mean embeddings in MMD. Hence, the quality of the prototypes selected from the proposed OT based approach can be expected to be superior compared to those using the MMD measure and is observed in all our experimental results.

We propose an OT based approach for searching a subset P from a source dataset X (i.e., $P \subset X$) that best represents a target set Y . In the special case where both the source and the target are the same set ($X = Y$), the prototypes in P represent a compact summary of X . We employ the Wasserstein distance to estimate the closeness between the distribution representing a candidate set P and set Y . Unlike the typical OT setting, the source distribution (representing P) in our problem setting is unknown and needs to be learned along with the transport plan. Hence, we model the prototype selection problem as learning an empirical source distribution p (representing set X) that has the minimal Wasserstein distance with the empirical target distribution (representing set Y). Since searching for the best prototypical set typically comes with a cardinality constraint, we constrain p to have a small support set (which represents $P \subset X$). The learned distribution p is also indicative of the relative importance of the prototypes in P in representing Y .

Our main contributions are as follows.

- We propose a novel unsupervised prototype selection algorithm based on the OT theory.
- We prove that the objective function of the proposed optimization is submodular, which leads to a tight approximation guarantee of $(1 - e^{-1})$ using greedy approximation algorithms (Nemhauser et al., 1978). We show that the computations in the proposed greedy algorithm can be parallelized, leading to a highly efficient implementation.
- Our empirical results show that the proposed algorithm outperforms existing baselines on several real-world datasets. The optimal transport framework allows our approach to seamlessly work in settings where the source (X) and the target (Y) datasets are from different domains.

The outline of the paper is as follows. We provide a brief review of the optimal transport setting, the prototype selection setting, and key results in the submodular optimization literature in Section 2. The proposed OT based prototype selection approach is presented in Section 3. We discuss how the proposed approach relates to existing works in Section 4. The empirical results are presented in Section 5. We conclude the paper and discuss promising directions of future work in Section 6.

2 Background

We begin by discussing the optimal transport problem.

2.1 Optimal transport

Let p and q be two probability measures over metric spaces \mathcal{X} and \mathcal{Y} and let a function $c : \mathcal{X} \times \mathcal{Y} \rightarrow \mathbb{R}_+$: $(\mathbf{x}, \mathbf{y}) \rightarrow c(\mathbf{x}, \mathbf{y})$ represents the *cost* of transporting a unit mass from $\mathbf{x} \in \mathcal{X}$ to $\mathbf{y} \in \mathcal{Y}$. Then, the optimal transport problem due to Kantorovich (1942) aims at finding a transport plan γ (with the minimal transporting effort) as a solution to the problem

$$\inf_{\gamma \in \Gamma(p, q)} \int_{\mathcal{X} \times \mathcal{Y}} c(\mathbf{x}, \mathbf{y}) d\gamma(\mathbf{x}, \mathbf{y}), \quad (1)$$

where $\Gamma(p, q)$ is the set of joint distributions with marginals p and q .

In several applications, the marginals p and q are not available. However, independent and identically distributed samples $X := \{\mathbf{x}_i\}_{i=1}^m$ and $Y := \{\mathbf{y}_j\}_{j=1}^n$ are available from distributions p and q , respectively. Let $\mathbf{C} \in \mathbb{R}_+^{m \times n}$ be the corresponding cost matrix, where $\mathbf{C}_{ij} = c(\mathbf{x}_i, \mathbf{y}_j)$. In such settings, commonly referred to as statistical OT, the empirical distributions may be employed:

$$p := \sum_{i=1}^m \mathbf{p}_i \delta_{\mathbf{x}_i}, \quad q := \sum_{j=1}^n \mathbf{q}_j \delta_{\mathbf{y}_j}, \quad (2)$$

where the probability associated with samples \mathbf{x}_i and \mathbf{y}_j are \mathbf{p}_i and \mathbf{q}_j , respectively, and δ is the Dirac delta function. The vectors \mathbf{p} and \mathbf{q} lie on simplices Δ_m and Δ_n , respectively, where $\Delta_k := \{\mathbf{z} \in \mathbb{R}_+^k \mid \sum_i \mathbf{z}_i = 1\}$. The OT problem (1) now simplifies to the popular discrete OT problem:

$$\min_{\gamma \in \Gamma(\mathbf{p}, \mathbf{q})} \langle \mathbf{C}, \gamma \rangle, \quad (3)$$

where $\Gamma(\mathbf{p}, \mathbf{q}) := \{\gamma \in \mathbb{R}_+^{m \times n} \mid \gamma \mathbf{1} = \mathbf{p}; \gamma^\top \mathbf{1} = \mathbf{q}\}$. Here, $\mathbf{0}$ and $\mathbf{1}$ are vectors of 0 and 1, respectively, of appropriate dimensions. The optimal transport metric (3) is also known as the earth mover's distance (Rubner et al., 2000).

The optimization problem (3) is a linear program. Recently, (Cuturi, 2013) proposed an efficient solution for learning entropy regularized transport plan γ in (3) using the Sinkhorn algorithm (Knight, 2008). For a recent survey on OT with focus on machine learning applications, please refer to (Peyré & Cuturi, 2019).

2.2 Prototype selection

Selecting representative elements is often posed as identifying a subset P from a set of items X (e.g., data points, features, etc.). The quality of selection is usually governed via a scoring function $f(P)$, which

encodes the desirable properties of prototypical samples. For instance, in order to obtain a compact yet informative subset P , the scoring function should discourage redundancy.

Recent works (Kim et al., 2016; Gurumoorthy et al., 2019) have posed prototype selection within the submodular optimization setting. They propose greedy algorithms that effectively evaluate the *incremental* benefit of adding an element in the prototypical set P . While (Kim et al., 2016; Gurumoorthy et al., 2019) propose MMD based scoring functions, to the best of our knowledge, ours is the first work which leverages the optimal transport (OT) framework to extract such compact representation. We prove that the proposed objective function is submodular, which ensures tight approximation guarantee using greedy approximate algorithms.

2.3 Submodularity

We now briefly review the concept of submodular and weakly submodular functions, which we later use to prove that the proposed objective for prototype selection is a submodular function.

Submodularity and Monotonicity Consider any two sets $A \subseteq B \subseteq [m]$. A set function $f(\cdot)$ is *submodular* if and only if for any $i \notin B$, $f(A \cup i) - f(A) \geq f(B \cup i) - f(B)$. The function is called *monotone* when $f(A) \leq f(B)$.

Submodularity implies diminishing returns property where the incremental gain in adding a new element i to a subset A is at least as high as adding to a superset B Fujishige (2005). An equivalent characterization of submodularity is via the submodularity ratio Elenberg et al. (2018); Das & Kempe (2011) defined as follows.

Submodularity Ratio Given two disjoint sets L and S , and a set function $f(\cdot)$, the submodularity ratio of $f(\cdot)$ for the ordered pair (L, S) is given by:

$$\alpha_{L,S} := \frac{\sum_{i \in S} [f(L \cup \{i\}) - f(L)]}{f(L \cup S) - f(L)}. \quad (4)$$

Submodularity ratio captures the increment in $f(\cdot)$ by adding the entire subset S to L , compared to summed gain of adding its elements individually to L . It is known that $f(\cdot)$ is submodular if and only if $\alpha_{L,S} \geq 1, \forall L, S$. In the case where $0 \leq \epsilon \leq \alpha_{L,S} < 1$ for an independent constant ϵ , $f(\cdot)$ is called *weakly submodular* Das & Kempe (2011).

We further define submodularity ratio of a set P with respect to an integer s as follows:

$$\alpha_{P,s} := \max_{\substack{L,S:L \cap S = \emptyset, \\ L \subseteq P, |S| \leq s}} \alpha_{L,S}. \quad (5)$$

It should be emphasized that unlike the definition in (Elenberg et al., 2018, Equation 3), the above Equation (5) involves the \max operator instead of the \min . This specific form is later used to produce approximation bounds for the proposed approach (presented in Algorithm 1). Both (strongly) submodular and weakly submodular functions enjoy provable performance bounds when the set elements are selected incrementally and greedily Nemhauser et al. (1978); Elenberg et al. (2018); Gurumoorthy et al. (2019).

3 Prototype selection using optimal transport theory

We begin by discussing how to pose prototype selection as an optimal transport (OT) problem.

3.1 Problem formulation

Let $X = \{\mathbf{x}_i\}_{i=1}^m$ be a set of m source points, $Y = \{\mathbf{y}_j\}_{j=1}^n$ be a target set of n data points, and $\mathbf{C} \in \mathbb{R}_+^{m \times n}$ represents the ground cost matrix. Our aim is to select a small, weighted subset $P \subset X$ of size $k \ll m$ that best describes Y . Traditionally, OT is defined as a minimization problem over the transport plan γ as in (3). In our setting, we pre-compute a *similarity* matrix $\mathbf{S} \in \mathbb{R}_+^{m \times n}$ from \mathbf{C} , for instance, as $\mathbf{S}_{ij} = \beta - \mathbf{C}_{ij}$ where $\beta > \|\mathbf{C}\|_\infty$. This allows to equivalently represent the OT problem (3) as a maximization problem with the objective function as $\langle \mathbf{S}, \gamma \rangle$. Treating it as a maximization problem enables to establish connection with submodularity and leverage standard greedy algorithms for its optimization with cardinality constraints (Nemhauser et al., 1978).

We propose to pose the problem of selecting a prototypical set (of utmost size k) as learning a sparse support empirical source distribution $w = \sum_{\mathbf{x}_i \in P} \mathbf{w}_i \delta_{\mathbf{x}_i}$ that has maximum closeness to the target distribution in terms of the optimal transport measure. Here, the weight $\mathbf{w} \in \Delta_m$ denotes the relative importance of the samples and the support of distribution w (or equivalently of the corresponding vector \mathbf{w}) is the set $\text{supp}(\mathbf{w}) = \{i : \mathbf{w}_i > 0\}$. Hence, the constraint $|P| \leq k$ for the prototype set P translates to $|\text{supp}(\mathbf{w})| \leq k$ or $(\|\mathbf{w}\|_0 \leq k)$ where $\text{supp}(\mathbf{w}) \subseteq P$.

We measure the suitability of a candidate prototype set $P \subset X$ with an OT based measure on sets. To elaborate, index the elements in X from 1 to m and let $[m] := \{1, 2, \dots, m\}$ denote the first m natural numbers. Given any index set of prototypes $P \subseteq [m]$, define a set function $f : 2^{[m]} \rightarrow \mathbb{R}_+$ as:

$$f(P) := \max_{\mathbf{w} : \text{supp}(\mathbf{w}) \subseteq P} \max_{\gamma \in \Gamma(\mathbf{w}, \mathbf{q})} \langle \mathbf{S}, \gamma \rangle, \quad (6)$$

where $\mathbf{q} \in \Delta_n$ corresponds to the (given) weights of the target samples¹ in the empirical target distribution q as in (2). The learned transport plan γ in (6) provides similarity information between the elements in P and Y , which is useful in several downstream applications (e.g., via barycentric mapping). Our goal is to find that set P that maximizes $f(\cdot)$ subject to the cardinality constraint, i.e.,

$$P^* = \arg \max_{P \subseteq [m], |P| \leq k} f(P). \quad (7)$$

The entries of optimal weight vector \mathbf{w}^* corresponding to P^* in (7) indicate the importance of the prototypes in summarizing set Y .

We would like to highlight the following differences from the standard OT setting (3):

- the source distribution w is learned as a part of the optimization, and
- the source distribution w is enforced to have a sparse support of utmost size k so that the prototypes create a compact summary.

In the next section, we analyze the objective function in (7), characterize it with a few desirable properties, and develop a computationally efficient greedy approximation algorithm.

3.2 Optimization algorithm and analysis

Though the definition of the scoring function $f(\cdot)$ in (6) involves maximization over two coupled variables \mathbf{w} and γ , it can be reduced to an equivalent optimization problem involving only γ (by eliminating \mathbf{w} altogether). To this end, let $k = |P|$ and denote \mathbf{S}_P a $k \times n$ sub-matrix of \mathbf{S} containing only those rows indexed by P . We then have the following lemma:

¹In the absence of domain knowledge, uniform weights $\mathbf{q} = \mathbf{1}/n$ can be considered a default choice.

Lemma 3.1. *The set function $f(\cdot)$ in (6) can be equivalently defined as an optimization problem only over the transport plan as follows:*

$$f(P) = \max_{\gamma \in \Gamma_P(\mathbf{q})} \langle \mathbf{S}_P, \gamma \rangle, \quad (8)$$

where $\Gamma_P(\mathbf{q}) := \{\gamma \in \mathbb{R}_+^{k \times n} \mid \gamma^\top \mathbf{1} = \mathbf{q}\}$. Let γ^* be an optimal solution of (8). Then, (\mathbf{w}^*, γ^*) is an optimal solution of (6) where $\mathbf{w}^* = \gamma^* \mathbf{1}$.

A closer look into the set function in (8) reveals that the optimization for γ can be done in parallel over the n target points, and its solution assumes a closed-form expression. It is worth noting that the constraint $\gamma^\top \mathbf{1} = \mathbf{q}$ as well as the objective $\langle \mathbf{S}_P, \gamma \rangle$ decouple over each column of γ . Hence, (8) can be solved across the columns of variable γ independently, thereby allowing parallelism over the target set. In other words,

$$f(P) = \sum_{j=1}^n \max_{\gamma^j \in \mathbb{R}_+^k} \langle \mathbf{S}_P^j, \gamma^j \rangle, \text{ s.t. } \mathbf{1}^T \gamma^j = \mathbf{q}_j \quad \forall j, \quad (9)$$

where \mathbf{S}_P^j and γ^j denote the j^{th} column vectors of the matrices \mathbf{S}_P and γ , respectively. Further, if i_j denotes the location of the maximum value in the vector \mathbf{S}_P^j , then an optimal solution for γ can be easily seen to inherit an extremely sparse structure with exactly one non-zero element on each column j at the row location i_j , i.e., $\gamma_{i_j, j} = \mathbf{q}_j, \forall j$ and 0 everywhere. The above important observation makes the solving (9) particularly suited to general purpose GPU computation. In addition, due to this specific solution structure in γ , determining the function value for any incremental set is a relatively inexpensive operation as presented in our next result.

Lemma 3.2 (Fast, parallelizable incremental computation). *Given any set P and its function value $f(P)$, the value at the incremental selection $f(P \cup S)$ obtained by adding $s = |S|$ new elements to P , can be computed in $O(sn)$ via a sequential implementation. If there are n nodes working in parallel, $f(P \cup S)$ can be obtained in $O(s)$ per node.*

Remark By setting $P = \emptyset$ and $f(\emptyset) = 0$, $f(S)$ for any set S can be computed efficiently as discussed in Lemma 3.2.

In addition to fast computation, the function $f(\cdot)$ in (8) enjoys the following desirable properties.

Theorem 3.3 (Submodularity). *The set function $f(\cdot)$ defined in (8) is monotone and submodular.*

Though obtaining the global optimum subset P^* in (7) of cardinality utmost k is a NP-complete problem, the submodularity of $f(\cdot)$ enables to provide provable approximation bounds for greedy element selections.

To this end, we present our method (henceforth termed as OTGreedy) detailed in Algorithm 1. The algorithm begins by setting the current selection $P = \emptyset$. Without loss of generality, we assume $f(\emptyset) = 0$ as $f(\cdot)$ is monotonic. In each iteration, it determines those s elements from the remainder set $[m] \setminus P$, denoted by S , that when individually added to P result in maximum incremental gain. This can be implemented efficiently as discussed in Lemma 3.2. Here $s \geq 1$ is the user parameter that decides the number of elements chosen in each iteration. The set S is then added to P . The algorithm proceeds for $\lceil \frac{k}{s} \rceil$ iterations to select k prototypes. As function $f(\cdot)$ in (8) is both monotone and submodular, it has the characteristic of diminishing returns. Hence, an alternative stopping criterion could be the minimum expected increment ϵ in the function value at each iteration. The algorithm stops when the increment in the function value is below the specified threshold ϵ .

Algorithm 1 OTGreedy

Input: sparsity level k or lower bound ϵ on increase in $f(\cdot)$, X , Y , s

Initialize $P = \emptyset$

while termination condition is false **do**

 {i.e., $|P| \leq k$, else increase in objective value $\geq \epsilon$.}

$\forall i \in [m] \setminus P$, let $\mathbf{v}_i = f(P \cup \{i\}) - f(P)$ forming the components of vector \mathbf{v}

$S =$ Set of indices of top s largest elements in \mathbf{v} .

$P = P \cup S$

end while

$\gamma_P = \arg \max_{\gamma \in \Gamma_P(\mathbf{q})} \langle \mathbf{S}_P, \gamma \rangle$

$\mathbf{w}_P = \gamma_P \mathbf{1}$

Return P , \mathbf{w}_P

Approximation guarantee for the OTGreedy algorithm: We first note the following result on the upper bound on the submodularity ratio (4). Let $s = |S|$. When $f(\cdot)$ is monotone, then

$$\alpha_{L,S} \leq \frac{\sum_{i \in S} [f(L \cup \{i\}) - f(L)]}{\max_{i \in S} [f(L \cup \{i\}) - f(L)]} \leq s \quad (10)$$

and hence $\alpha_{P,s} \leq s$. In particular, $s = 1$ implies $\alpha_{P,1} = 1$, as for any $L \subseteq P$, $\alpha_{L,S} = 1$ when $|S| = 1$. Our next result provides the performance bound for the proposed OTGreedy algorithm.

Theorem 3.4 (Performance bounds for OTGreedy). *Let P be the final set returned by the OTGreedy method described in Algorithm 1. Let $\alpha = \alpha_{P,s}$ be the submodularity ratio of the set P w.r.t. s . If P^* is the optimal set of k elements that maximizes $f(\cdot)$ in (7) then*

$$f(P) \geq f(P^*) \left[1 - e^{-\frac{1}{\alpha}}\right] \geq f(P^*) \left[1 - e^{-\frac{1}{s}}\right]. \quad (11)$$

When $s = 1$ we recover the known approximation guarantee of $(1 - e^{-1})$ [Nemhauser et al. \(1978\)](#).

4 Related works and discussion

As discussed earlier, recent works ([Kim et al., 2016](#); [Gurumoorthy et al., 2019](#)) view the unsupervised prototype selection problem as searching for a set $P \subset X$ whose underlying distribution is similar to the one corresponding to the target dataset Y . However, instead of the true source and target distributions, only samples from them are available. In such a setting, φ -divergences ([Csiszár, 1972](#)) such as total variation distance, KL-divergence, etc. require density estimation or space-partitioning/bias-correction techniques ([Smola et al., 2007](#); [Song, 2008](#)), which can be computationally prohibitive in higher dimensions. Moreover, they may be agnostic to the natural geometry of the ground metric. Maximum mean discrepancy (MMD) metric employed by ([Kim et al., 2016](#); [Gurumoorthy et al., 2019](#)), on the other hand, can be computed efficiently but does not faithfully lift ground metric of the samples ([Feydy et al., 2018](#)).

We propose an optimal transport (OT) based prototype selection approach. OT framework respects the intrinsic geometry of the space of the distributions. Moreover, there is an additional flexibility in the

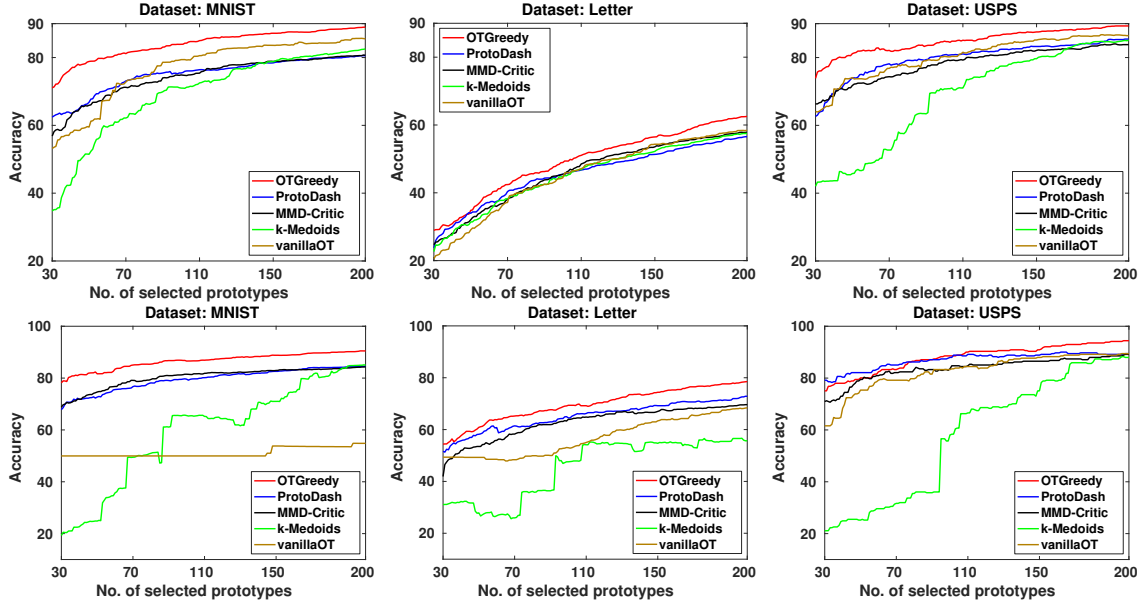


Figure 1: Performance of different algorithms for prototype selection on different datasets. The top row corresponds to the setting where all the classes (digit/letter) have uniform representation in the target set. The bottom row corresponds to the challenging skewed setting where a particular class (digit/letter) represents 50% of the target set (while the remaining classes together uniformly represent the remaining 50% of the target set).

choice of the ground metric, e.g., ℓ_1 -norm distance, which need not be a (universal) kernel induced function sans which the distribution approximation guarantees of MMD may no longer be applicable (Cortes et al., 2008; Gretton et al., 2012). Solving the classical OT problem (3) is known to be computationally more expensive than computing MMD. However, our setting differs from classical OT, as the source distribution is also learned in (6). As shown in Lemma 3.1, the joint learning of the source distribution and the optimal transport plan has an equivalent but computationally efficient reformulation (8). The solution structure of (8) can easily take advantage of GPU implementation due to parallelizable incremental computation.

Using OT is also favorable from a theoretical standpoint. Though the MMD function in (Kim et al., 2016) is proven to be submodular, it is only under restricted conditions like the choice of kernel matrix and equal weighting of prototypes. (Gurumoorthy et al., 2019) extends (Kim et al., 2016) by allowing for unequal weights and eliminating any additional conditions on the kernel, but forgoes submodularity as the resultant MMD objective could only be proven to be weakly submodular. In this backdrop, the proposed OT based objective (7) is a submodular function without requiring any further assumptions. It is worth noting that submodularity leads to a tighter approximation guarantee of $(1 - e^{-1})$ using greedy approximation algorithms Nemhauser et al. (1978), whereas the best greedy based approximation for weak submodular functions (submodularity ratio of $\alpha < 1$) is only $(1 - e^{-\alpha})$ Elenberg et al. (2018). A better theoretical approximation of the OT based subset selection encourages the selection of better quality prototypes.

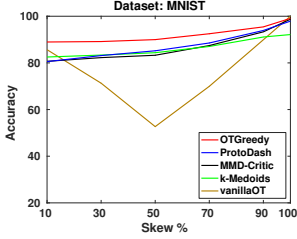


Figure 2: Comparisons of different algorithms in representing targets with varying skew percentage of a MNIST digit.

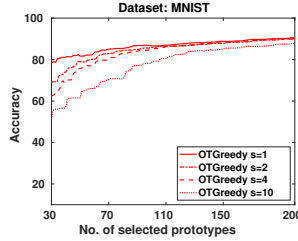


Figure 3: Performance of our OTGreedy algorithm with varying subset selection size s on the MNIST dataset.

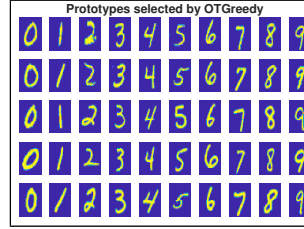


Figure 4: Prototypes selected by OTGreedy for the dataset containing one of the 10 MNIST digits (column-wise).

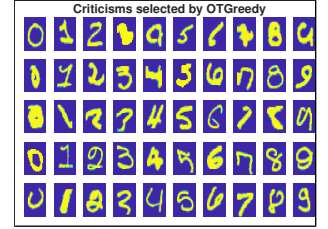


Figure 5: Criticisms chosen by OTGreedy for the dataset containing one of the 10 MNIST digits (column-wise).

5 Experiments

We evaluate the generalization performance and computational efficiency of the proposed OTGreedy algorithm against state-of-the-art on several real-world datasets. Our implementation is available at <https://pratikjawanpuria.com>.

5.1 Prototype selection within same domain

We validate the quality of representative samples selected by different prototype selection algorithms via the performance of the corresponding *nearest prototype classifier* (Bien & Tibshirani, 2011b; Kim et al., 2016; Gurumoorthy et al., 2019). Let X and Y represent source and target datasets containing instances from the same domain but (possibly) containing different class distributions. The aim is unsupervised selection of a subset $P \subseteq X$ that is representative of the target set Y . The quality of P is evaluated by classifying the target set instances with 1-nearest neighbour (1-NN) classifier parameterized by the elements in P . The class information of the samples in P is made available during this evaluation stage. Such a setting has potential application in transfer learning and covariate shift correction (Gurumoorthy et al., 2019). The following algorithms are evaluated along with OTGreedy (Algorithm 1):

- **MMD-Critic** (Kim et al., 2016) employs a MMD based scoring function. All the samples are weighted equally in the scoring function.
- **ProtoDash** (Gurumoorthy et al., 2019) employs a weighted MMD based scoring function. The learned weights indicate the importance of the samples.
- **k-Medoids** (Kaufman & Rousseeuw, 1987) is an unsupervised partitioning technique that selects actual data points as the centers (prototypes).

We additionally develop a fourth (novel) baseline **vanillaOT** using our framework. It solves the proposed problem (6) with $P = [m]$, i.e., no cardinality constraint. It then selects the top- k prototypes based on the weights \mathbf{w} obtained by solving (6). Hence, vanillaOT selects prototypes in a non-incremental fashion, unlike OTGreedy where the next selection depends upon the current selection of elements. The final transport plan for vanillaOT is obtained using (8).

We consider the following multi-class benchmarks:

- **MNIST** (LeCun et al., 1998) is a handwritten digit dataset consisting of greyscale images of digits $\{0, \dots, 9\}$. The images are of 28×28 pixels.
- **Letter** dataset (Dua & Graff, 2017) consists of images of 26 capital letters of the English alphabets. Each letter is represented as a 16 dimensional feature vector.
- **USPS** dataset (Hull, 1994) consists of handwritten greyscale images of $\{0, \dots, 9\}$ digits represented as 16×16 pixels.

Experimental setup: In the first set of experiments, all the classes are equally represented in the target set (corresponding to each dataset). In second set of experiments, the target sets are constructed such that they are skewed towards a randomly chosen class, whose instances (digit/letter) form $z\%$ of the target set and the instances from the other classes uniformly constitute the remaining $(100 - z)\%$ of the target set. For a given dataset, the source set is same for all the experiments and uniformly represents all the classes. The algorithms select up to top 200 prototypes in each experiment. More details such as the size of source and target datasets, etc., are available in the supplementary material.

Results: Figure 1 (top row) shows the results of the first set of experiments on the three datasets. We plot the test set accuracy for a range of top- k prototypes selected. In general, we observe that the proposed OTGreedy performs much better than the baselines. Figure 1 (bottom row) shows the results when samples of a (randomly chosen) class constitutes 50% of the target set. OTGreedy again outperforms the baselines in this challenging setting. We observe that in several instances, OTGreedy opens up a significant performance gap even with only a few selected prototypes. Figure 2 shows that OTGreedy achieves the best performance on different skewed versions of the MNIST dataset (with $k = 200$). Interestingly, in cases where target is either uniform or heavily skewed, even non-incremental algorithms like vanillaOT can select prototypes that match target distribution. However, in the harder setting when the skew varies from 20% to 80%, vanillaOT predominantly selects the skewed class leading to poor performance. The running time of algorithms on the MNIST dataset are: 5.3s (OTGreedy), 8.6s (ProtoDash), 5.9s (MMD-Critic), 184.5s (k-Medoids), and 0.04s (vanillaOT).

In Figure 3, we plot the performance of OTGreedy for different choices of value s specifying the number of elements chosen simultaneously in each iteration, for the setting where the target has 50% skew of one of the MNIST digit. Recall that increasing s proportionally decreases the computational time at the cost of generalization performance. The number of iterations $\lceil \frac{k}{s} \rceil$ steadily decreases with increasing s , but choosing few elements simultaneously leads to better incremental selection in subsequent iterations. We note that between $s = 1$ and $s = 10$, the degradation in quality is only marginal even when we choose as few as 110 prototypes and the performance gap continuously narrows with increasing selection of prototypes. However, the time taken by OTGreedy with $s = 10$ is 0.54s, which is the expected 10x speedup compared to OTGreedy with $s = 1$.

Identifying criticisms: Following the procedure outlined in Section 3.2 of Kim et al. (2016), we further make use of the prototypes selected by OTGreedy to identify *criticisms*. These are data points belonging to the region of input space not well explained by prototypes and are farthest away from them. We use a witness function similar to (Kim et al., 2016, Section 3.2). The columns of Figure 5 visualizes the few chosen criticisms, one for each of the 10 datasets containing samples of the respective MNIST digits. It is evident that the selected data points are indeed outliers for the corresponding digit class. Since the criticisms are those points that are maximally dissimilar from the prototypes, it is also a reflection on how well the prototypes of OTGreedy represent the underlying class as seen in Figure 4, where in each column we plot the selected prototypes for a dataset comprising one of the 10 digits.

Table 1: Accuracy obtained on the Office-Caltech dataset.

Task	MMD-Critic	MMD-Critic+OT	ProtoDash	ProtoDash+OT	k-Medoids	k-Medoids+OT	vanillaOT	OTGreedy
$A \rightarrow C$	73.98	78.16	70.23	72.28	78.25	75.40	82.62	83.60
$A \rightarrow D$	75.16	72.61	77.71	71.97	77.71	69.43	80.25	82.80
$A \rightarrow W$	51.53	62.71	48.81	58.64	63.73	69.49	62.37	75.59
$C \rightarrow A$	83.71	86.17	83.82	87.25	81.99	81.89	71.92	90.03
$C \rightarrow D$	70.06	75.16	71.34	70.70	82.80	76.43	75.80	89.17
$C \rightarrow W$	49.83	54.92	46.44	53.56	66.78	68.81	70.85	82.03
$D \rightarrow A$	82.85	85.21	83.39	83.82	80.39	76.53	91.00	90.89
$D \rightarrow C$	78.25	78.34	75.40	79.41	73.44	76.29	85.38	86.27
$D \rightarrow W$	80.00	84.41	85.08	86.10	86.78	87.12	75.59	92.20
$W \rightarrow A$	71.60	78.56	68.38	74.71	70.31	72.99	87.03	84.99
$W \rightarrow C$	67.20	75.76	65.86	74.60	65.24	71.93	74.06	83.12
$W \rightarrow D$	92.36	96.18	88.54	89.81	89.17	83.44	86.62	94.90
Average	73.04	77.35	72.08	75.24	76.38	76.08	78.36	86.30

5.2 Prototype selection from different domains

We next consider a setting where the source and target datasets contain instances from different domains. We experiment on the Office-Caltech dataset (Gong et al., 2012), which has images from four domains: Amazon (online website), Caltech (image dataset), DSLR (images captured using a high resolution DSLR camera), and Webcam (images captured using a webcam). Each domain has images from ten given classes. However, images from the same class across domains vary due to several factors such as different background, lighting conditions, etc. The number of data points in each domain is: 958 (A: Amazon), 1123 (C: Caltech), 157 (D: DSLR), and 295 (W: Webcam). The number of instances per class per domain ranges from 8 to 151.

We design similar experiment as in Section 5.1 by considering each domain, in turn, as the source or the target. Thus, there are twelve different tasks where task $A \rightarrow W$ implies that Amazon and Webcam are the source and the target domains, respectively. Since we use the DeCAF6 deep features of size 4096 to represent all the images (Donahue et al., 2014; Courty et al., 2017), the domains share the same feature space. However, compared to Section 5.1, this is a more challenging setting since both sample and feature distributions vary across domains.

Results: Table 1 reports the accuracy obtained on every task. We observe that our OTGreedy significantly outperforms the baselines MMD-Critic, ProtoDash, and k-Medoids. This is because OTGreedy learns both the prototypes as well as the transport plan between the prototypes and the target set instances. The transport plan allows the prototypes to be transported to the target domain via the barycentric projection, a characteristic of the optimal transport framework. OTGreedy is also much better than vanillaOT due to its superior incremental nature of prototype selection.

We also empower the three non-OT based baselines for the domain adaptation setting as follows. After selecting the prototypes via a baseline, we learn an OT plan between the selected prototypes and the target data points by solving the OT problem (3). The distribution of the prototypes is taken to be the normalized weights obtained by the baseline. This ensures that the prototypes selected by MMD-Critic+OT, ProtoDash+OT, and k-Medoids+OT are also transported to the target domain. Though we observe marked improvements in the performance of MMD-Critic+OT and ProtoDash+OT, the proposed OTGreedy still outperforms them. Overall, the above results illustrates the effectiveness of jointly selecting the prototypes and learning the transport plan, as done the proposed OTGreedy algorithm.

6 Conclusion

We have looked at the prototype selection problem from the viewpoint of optimal transport. In particular, we show that the problem is equivalent to learning a sparse source distribution w , whose probability values w_i specify the relevance of the corresponding prototype in representing the given target set. After establishing connections with submodularity, we proposed the OTGreedy algorithm that employs incremental greedy selection of prototypes and comes with (i) deterministic theoretical guarantees, (ii) simple implementation with updates that are amenable to parallelization, and (iii) excellent performance on different benchmarks.

Future works: We list a few interesting generalizations and research directions worth pursuing.

- We note that the proposed k -prototype selection problem (6) may be viewed as learning an ℓ_0 -norm regularized (fixed-support) Wasserstein barycenter of a single distribution. Extending it to the general ℓ_0 -norm regularized (fixed-support) Wasserstein barycenter of multiple distributions may be useful in applications like model compression, noise removal, etc.
- With the Gromov-Wasserstein (GW) distance (Mémoli, 2011; Peyré et al., 2016), the OT distance has been extended to settings where the source and the target distributions do not share the same feature and metric space. Our OT based prototype selection framework can be extended with the GW-distances for selecting prototypes when source and target domain share similar concepts/categories/classes but are defined over different feature spaces.

A Proof of theoretical results proposed in the main paper

A.1 Proof of Lemma 3.1

Since $\text{supp}(\mathbf{w}) \subseteq P$, (6) can be equivalently stated as:

$$f(P) := \max_{\mathbf{w}} \max_{\gamma \in \Gamma(\mathbf{w}, \mathbf{q})} \langle \mathbf{S}_P, \gamma \rangle, \quad (12)$$

where the optimization for the transport plan γ is over dimensions $k \times n$ and \mathbf{w} is of length k . Let (\mathbf{w}^f, γ^f) be the point of maximum for $f(P)$. For the function $g(P) = \max_{\gamma \in \Gamma_P(\mathbf{q})} \langle \mathbf{S}_P, \gamma \rangle$, let the maximum occur at γ^g .

Define $\mathbf{w}^g = \gamma^g \mathbf{1}$. Observe that $\|\mathbf{w}^g\|_1 = \sum_{i=1}^m \sum_{j=1}^n \gamma_{i,j}^g = \sum_{j=1}^n \mathbf{q}_j = 1$. Further as $\mathbf{w}_i^g \geq 0$ and $\text{supp}(\mathbf{w}^g) \subseteq P$, it is feasible source distribution in the optimization for $f(P)$. Assume $\gamma^f \neq \gamma^g$. We consider three different cases.

case 1: Let $f(P) = g(P)$. Then (\mathbf{w}^g, γ^g) also maximizes $f(P)$ proving that both the optimization problems are equivalent.

case 2: Let $f(P) < g(P)$. Then (\mathbf{w}^f, γ^f) cannot be the point of maximum as the value of the objective $\langle \mathbf{S}_P, \gamma^g \rangle$ in (12), evaluated at the feasible point (\mathbf{w}^g, γ^g) , is higher than $\langle \mathbf{S}_P, \gamma^f \rangle$.

case 3: Let $f(P) > g(P)$. Then γ^g cannot be the maximum point for $g(P)$ as it can be further maximized by selecting the transport plan γ^f .

Hence $f(P) = g(P)$ and the proof follows.

A.2 Proof of Lemma 3.2

Define a function $f^j(P)$ for each term in the decoupled form stated in (9), namely

$$f^j(P) := \max_{\gamma^j \in \mathbb{R}_+^k} \langle \mathbf{S}_P^j, \gamma^j \rangle, \text{ s.t. } \mathbf{1}^T \gamma^j = \mathbf{q}_j \quad (13)$$

so that $f(P) = \sum_{j=1}^n f^j(P)$. Based on the solution structure of γ^j discussed in Section 3.2, $f^j(P) = \Delta_P^j \mathbf{q}_j$ where Δ_P^j is the maximum value in the vector \mathbf{S}_P^j . Note that $\Delta_{P \cup S}^j = \max(\Delta_P^j, \Delta_S^j)$. Computing Δ_S^j is an $O(s)$ operation requiring to identify the maximum value of s elements. Given $f(P)$ (and $\Delta_P^j, \forall j$), $\Delta_{P \cup S}^j$ for each j can be computed independently of each other in $O(s)$ and the lemma follows.

A.3 Proof of Theorem 3.3

Consider the definition of $f^j(P)$ in (13). Recall that $f(P) = \sum_{j=1}^n f^j(P)$. As sums of monotone and submodular functions are also respectively monotone and submodular Fujishige (2005), it is sufficient to prove that $f^j(P)$ inherits these characteristics.

Consider any two sets $A \subseteq B$. As $\Delta_A^j \leq \Delta_B^j$, we have $f^j(A) \leq f^j(B)$ proving that it is monotone. For any $i \notin B$, let $\hat{A} = A \cup \{i\}$ and $\hat{B} = B \cup \{i\}$. If $\Delta_B^j > \Delta_{\hat{B}}^j$, then the maximum value in the j^{th} column vector *strictly increases* by adding the element i . Hence $\Delta_{\hat{A}}^j = \Delta_{\hat{B}}^j$. It then follows that $\Delta_{\hat{A}}^j - \Delta_A^j \geq \Delta_{\hat{B}}^j - \Delta_B^j$ proving that it is submodular.

A.4 Proof of Theorem 3.4

Let $t = \frac{k}{s}$ be the total number of iterations executed by OTGreedy. Without loss of generality we assume s divides k . Denote P_i as the set chosen at the end of iteration i such that the final set $P = P_t$. Let $P_{i+1} = P_i \cup S_{i+1}$ created by adding the s new elements in S_{i+1} to P_i during the iteration $i + 1$. Define the residual set $P_R = P^* \setminus P_i$. Since S_{i+1} contains the top s elements that results in the maximum incremental gain, we have

$$\frac{\sum_{e \in S_{i+1}} [f(P_i \cup \{e\}) - f(P_i)]}{s} \geq \frac{\sum_{e \in P_R} [f(P_i \cup \{e\}) - f(P_i)]}{k},$$

where we have used the fact that $|P_R| \leq k$. Based on the definition of submodularity ratio in (4) and $\alpha = \alpha_{P,s}$ in (5), and recalling that $P_i \subseteq P$, we get

$$\begin{aligned} f(P_{i+1}) - f(P_i) &\geq \frac{1}{\alpha} \sum_{e \in S_{i+1}} [f(P_i \cup \{e\}) - f(P_i)] \\ &\geq \frac{1}{\alpha} \frac{s}{k} [f(P_i \cup P_R) - f(P_i)]. \end{aligned} \tag{14}$$

The last inequality in (14) follows from the fact that submodularity ratio of $f(\cdot)$ for the ordered pair (P_i, P_R) is lower bounded by 1. As $f(\cdot)$ is monotone and $P^* \subseteq P_i \cup P_R$, we get $f(P^*) \leq f(P_i \cup P_R)$. Setting $\beta_i = f(P^*) - f(P_i)$ we can express $f(P_{i+1}) - f(P_i) = \beta_i - \beta_{i+1}$. Putting all this together and letting $\kappa = \frac{s}{k} \frac{1}{\alpha}$, the increment at the iteration $i + 1$ respects the inequality $\beta_i - \beta_{i+1} \geq \kappa \beta_i$, leading to the recurrence relation: $\beta_{i+1} \leq (1 - \kappa) \beta_i$. When iterated t times from step 0 and noting that $\beta_0 = f(P^*)$ and $\beta_t = f(P^*) - f(P)$, we have

$$f(P) \geq f(P^*) [1 - (1 - \kappa)^t].$$

Using the relation $1 - \kappa \leq e^{-\kappa}$ for all $\kappa \geq 0$ we have the required approximation guarantee:

$$f(P) \geq f(P^*) [1 - e^{-\kappa t}] \geq f(P^*) \left[1 - e^{-\frac{1}{\alpha}}\right].$$

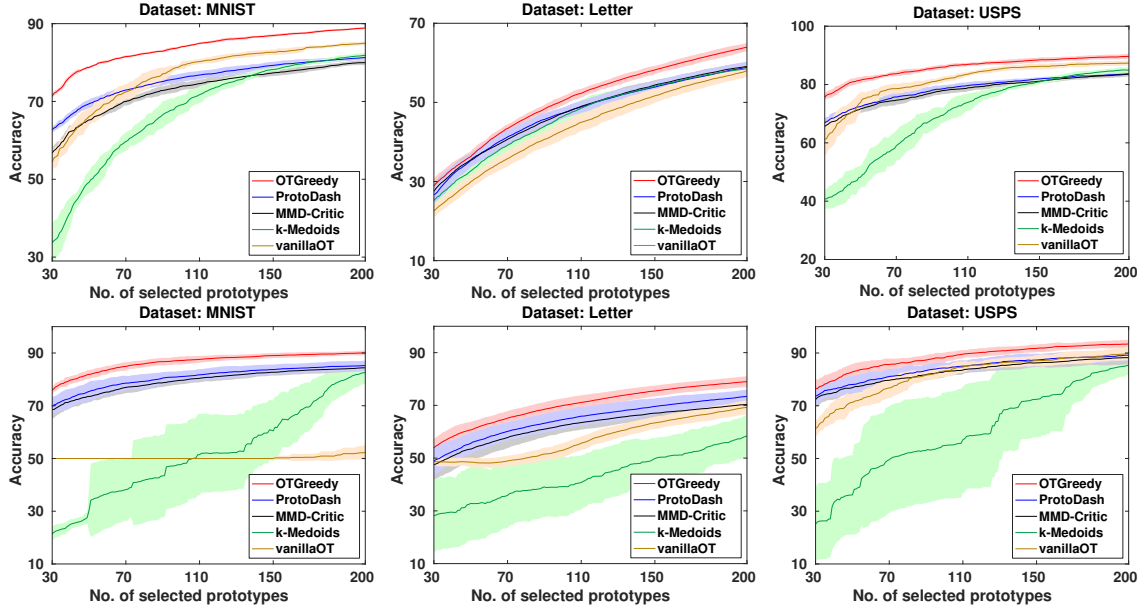


Figure 6: [Top row] Average performance of different algorithms for prototype selection on different datasets in the setting where all the classes uniformly represents the target set. The standard deviation for every k is represented as a lighter shaded band around the mean curve corresponding to each method. [Bottom row] Average performance of different algorithms for prototype selection on different datasets in the skewed setting where a particular class (digit/letter) represents 50% of the target set while the remaining classes together uniformly represent the remaining 50% of the target set. The results are averaged over different runs in which each class, in turn, is skewed. The standard deviation for every k is represented as a lighter shaded band around the mean curve corresponding to each method.

B Datasets and baseline details

In this section, we present the details such as size of the source/target datasets and cross-validation on the hyper-parameters of the baselines. We begin with the dataset details:

- **MNIST**²: It consists of two different sets of sizes $60K$ and $10K$ respectively. Following (Gurumoorthy et al., 2019), we randomly sampled $5K$ points from the $10K$ set and created the source set X . This source set is kept unchanged for all the (MNIST) experiments. The target set Y , constructed as a subset of $60K$, varies with the skew of the randomly chosen class c . The instances from c form $z = \{10, 30, 50, 70, 100\}$ percent of Y and the instances from other classes uniformly constitute the remaining $(100 - z)\%$ of Y . The most frequent class in the MNIST training set has 6742 elements while the least frequent class has 5421 instances. Hence, when $z = 10$, Y consists of 5421 randomly chosen data points of every class. For the case $z \geq 30$, the size of Y is appropriately adjusted in order that all the instances of class c exactly constitute the $z\%$ of Y . The instances of the other 9 classes are randomly chosen so that each of them account for $(100 - z)/9$ percent of Y .
- **Letter**³: it consists of 20 000 data points and has 26 classes. We randomly sample 4000 data points

²<http://yann.lecun.com/exdb/mnist>

³<https://archive.ics.uci.edu/ml/datasets/Letter+Recognition>

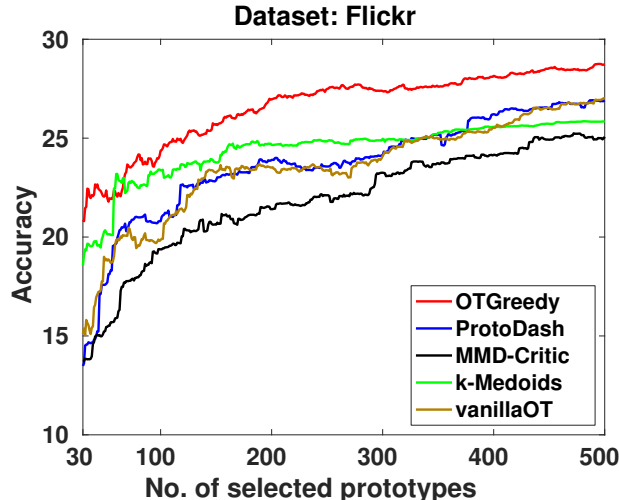


Figure 7: Performance of different algorithms for prototype selection on the Flickr dataset.

as the source set and the remaining data points are used to construct target sets (with different skews) as discussed above in the case of MNIST.

- **USPS**: the source set consist of 7291 data points. The target sets are constructed from the remaining 2007 data points, as discussed above in the case of MNIST.
- **Flickr** (Thomee et al., 2016) is the Yahoo/Flickr Creative Commons dataset consisting of descriptive tags of various real-world outdoor/indoor images. It should be noted that unlike MNIST, Letters, or USPS, Flickr is a multi-label tag-prediction dataset, i.e., each image can have multiple tags (labels) associated with it. The dataset and the image features, extracted using MatConvNet (Vedaldi & Lenc, 2015), are available at <http://cbcl.mit.edu/wasserstein>. The source and target sets consists of 9836 and 9885 data points, respectively, from 1000 tags (labels).

Following (Gurumoorthy et al., 2019), we use Gaussian kernels in all our experiments. The kernel-width is chosen by cross-validation from the set $\{0.1, 0.5, 1, 5, 10\}$. Our experiments are run on a machine with 6 core Intel CPU (3.60 GHz Xeon), 128 GB RAM, and a single NVIDIA Quadro M2000 GPU (4 GB). As discussed in the main paper, the quality of the representative elements selected by various methods is validated by the accuracy of the corresponding nearest prototype classifier.

C Additional experimental results

In Figure 1 top row (main paper), we discussed the results corresponding to the setting where the proportion of all the classes are same in equal in the target set. Figure 6 top row shows the results in this setting averaged over 10 randomized runs. The standard deviation (for every k) is represented as a shaded band around the mean. We observe that our OTGreedy algorithm obtains the best performance and has significantly more stable results across randomized runs than other methods.

In Figure 1 bottom row (main paper), we discussed the results corresponding to the setting where a randomly chosen class in the target set has 50% skew. We repeat this experiments for all the classes, i.e.,

each class in turn has 50% skew. This implies 10 runs for MNIST, 26 runs for Letters, and 10 runs for USPS. For each dataset, we average the results for each k (number of selected prototypes) and present it in Figure 6 bottom row. The standard deviation (for every k) is represented as a shaded band around the mean. Our OTGreedy algorithm outperforms other methods and has more stable results across runs in this challenging setting, illustrating the effectiveness of the proposed OT based framework.

Since Flickr is a multi-label dataset we report an accuracy metric, where a correct prediction is assigned if and only if one of the labels from the nearest labelled image (that is used for prediction) belongs to the set of ground-truth labels corresponding to the test image. Though the metric for prediction accuracy could appear to be conservative, it is worth emphasizing that in the backdrop 1000 possible different labels with an average of 5 labels per data point, a random nearest neighbour assignment will lead to correct prediction only with a probability of 0.0248 or accuracy of $\approx 2.5\%$. Figure 7 shows the result on the Flickr dataset. We observe that the proposed OTGreedy algorithm obtains the best result here as well.

References

- Arjovsky, M., Chintala, S., and Bottou, L. Wasserstein generative adversarial networks. In *ICML*, 2017.
- Bien, J. and Tibshirani, R. Hierarchical clustering with prototypes via minimax linkage. *Journal of the American Statistical Association*, 106(495):1075–1084, 2011a.
- Bien, J. and Tibshirani, R. Prototype Selection for Interpretable Classification. *Ann. Appl. Stat.*, 5(4): 2403–2424, 2011b.
- Caruana, R., Lou, Y., Gehrke, J., Koch, P., Sturm, M., and Elhadad, N. Intelligible models for healthcare. In *ACM conference on Knowledge Discovery and Data Mining (KDD)*, 2015.
- Cortes, C., Mohri, M., Riley, M., and Rostamizadeh, A. Sample selection bias correction theory. In *International Conference on Algorithmic Learning Theory*, 2008.
- Courty, N., Flamary, R., Habrard, A., and Rakotomamonjy, A. Joint distribution optimal transportation for domain adaptation. In *NeurIPS*, 2017.
- Courty, N., Flamary, R., Tuia, D., and Rakotomamonjy, A. Optimal transport for domain adaptation. *IEEE Transactions on Pattern Analysis and Machine Intelligence*, 39(9):1853–1865, 2017.
- Csiszár, I. A class of measures of informativity of observation channels. *Periodica Mathematica Hungarica*, 2(1):191–213, 1972.
- Cuturi, M. Sinkhorn distances: Lightspeed computation of optimal transport. In *NeurIPS*, 2013.
- Das, A. and Kempe, D. Submodular meets Spectral: Greedy Algorithms for Subset Selection, Sparse Approximation and Dictionary Selection. In *Intl. Conference on Machine Learning (ICML)*, 2011.
- Donahue, J., Jia, Y., Vinyals, O., Hoffman, J., Zhang, N., Tzeng, E., and Darrell, T. DeCAF: A deep convolutional activation feature for generic visual recognition. In *ICML*, 2014.
- Dua, D. and Graff, C. UCI machine learning repository, 2017. URL <http://archive.ics.uci.edu/ml>.

- Elenberg, E., Khanna, R., Dimakis, A. G., and Negahban, S. Restricted Strong Convexity Implies Weak Submodularity. *Ann. Stat.*, 46:3539–3568, 2018.
- Feydy, J., Séjourné, T., Vialard, F.-X., ichi Amari, S., Trounev, A., and Peyré, G. Interpolating between optimal transport and mmd using Sinkhorn divergences. In *AISTATS*, 2018.
- Frogner, C., Zhang, C., Mobahi, H., Araya-Polo, M., and Poggio, T. Learning with a wasserstein loss. In *NeurIPS*, 2015.
- Fujishige, S. *Submodular functions and optimization*. Number 58 in Annals of Discrete Mathematics. Elsevier Science, 2 edition, 2005.
- Gong, B., Shi, Y., Sha, F., and Grauman, K. Geodesic flow kernel for unsupervised domain adaptation. In *CVPR*, 2012.
- Gretton, A., Borgwardt, K. M., Rasch, M., Schölkopf, B., and Smola, A. J. A Kernel Method for the Two-Sample-Problem. In *20th Conference on Neural Information Processing Systems (NIPS)*, pp. 513–520, 2006.
- Gretton, A., Borgwardt, K. M., Rasch, M., Schölkopf, B., and Smola, A. J. A kernel two-sample test. *Journal of Machine Learning Research*, 13(25):723–773, 2012.
- Gurumoorthy, K. S., Dhurandhar, A., Cecchi, G., and Aggarwal, C. Efficient data representation by selecting prototypes with importance weights. In *19th IEEE International Conference on Data Mining (ICDM)*, 2019.
- Hull, J. J. A database for handwritten text recognition research. *IEEE Transactions on Pattern Analysis and Machine Intelligence*, 16(5):550–554, 1994.
- Idé, T. and Dhurandhar, A. Supervised Item Response Models for Informative Prediction. *Knowl. Inf. Syst.*, 51(1):235–257, 2017.
- Kantorovich, L. On the translocation of masses. *Doklady of the Academy of Sciences of the USSR*, 37: 199–201, 1942.
- Kaufman, L. and Rousseeuw, P. Clustering by means of medoids. *Statistical Data Analysis Based on the L1 Norm and Related Methods*, pp. 405—416, 1987.
- Kim, B., Rudin, C., and Shah, J. The Bayesian case model: A generative approach for case-based reasoning and prototype classification. In *NeurIPS*, 2014.
- Kim, B., Khanna, R., and Koyejo, O. Examples are not Enough, Learn to Criticize! Criticism for Interpretability. In *30th Conference on Neural Information Processing Systems (NIPS)*, 2016.
- Knight, P. A. The sinkhorn-knopp algorithm: Convergence and applications. *SIAM J. Matrix Anal. Appl.*, 30(1):261—275, 2008.
- Koh, P. W. and Liang, P. Understanding black-box predictions via influence functions. In *ICML*, 2017.
- LeCun, Y., Bottou, L., Bengio, Y., and Haffner, P. Gradient-based learning applied to document recognition. *Proceedings of the IEEE*, 86(11):2278–2324, November 1998.

- Lozano, M., Sotoca, J. M., Sánchez, J. S., Pla, F., Pkalska, E., and Duin, R. P. W. Experimental study on prototype optimisation algorithms for prototype-based classification in vector spaces. *Pattern Recogn.*, 39(10):1827–1838, 2006.
- Mémoli, F. Gromov-Wasserstein distances and the metric approach to object matching. *Foundations of Computational Mathematics*, 11(4):417–487, 2011.
- Nemhauser, G. L., Wolsey, L. A., and Fisher, M. L. An Analysis of Approximations for Maximizing Submodular Set Functions. *Math. Program.*, 14:265–294, December 1978.
- Peyré, G. and Cuturi, M. Computational optimal transport. *Foundations and Trends in Machine Learning*, 11(5-6):355–607, 2019.
- Peyré, G., Cuturi, M., and Solomon, J. Gromov-Wasserstein averaging of kernel and distance matrices. In *ICML*, 2016.
- Ribeiro, M., Singh, S., and Guestrin, C. ”Why Should I Trust You?” Explaining the Predictions of Any Classifier. In *ACM SIGKDD Intl. Conference on Knowledge Discovery and Data Mining (KDD)*, 2016.
- Rousseeuw, P. J. and Kaufman, L. *Finding Groups in Data: An Introduction to Cluster Analysis*. John Wiley & Sons, Inc., 2009.
- Rubner, Y., Tomasi, C., and Guibas, L. J. The earth mover’s distance as a metric for image retrieval. *International Journal of Computer Vision*, 40(2):99–121, 2000.
- Smola, A., Gretton, A., Song, L., and Schölkopf, B. A Hilbert space embedding for distributions. In *International Conference on Algorithmic Learning Theory*, 2007.
- Solomon, J., de Goes, F., Peyré, G., Cuturi, M., Butscher, A., Nguyen, A., Du, T., and Guibas, L. Convolutional Wasserstein distances: Efficient optimal transportation on geometric domains. *ACM Transactions on Graphics*, 34(4), 2015.
- Song, L. *Learning via Hilbert Space Embedding of Distributions*. PhD thesis, The University of Sydney, 2008.
- Thomee, B., Shamma, D. A., Friedland, G., Elizalde, B., Ni, K., Poland, D., Borth, D., and Li, L.-J. Yfcc100m: The new data in multimedia research. *Communications of ACM*, 59(2):64–73, 2016.
- Vedaldi, A. and Lenc, K. Matconvnet: Convolutional neural networks for matlab. In *ACM International Conference on Multimedia*, pp. 689–692, 2015.
- Villani, C. *Optimal Transport: Old and New*, volume 338. Springer Verlag, 2009.
- Wei, K., Iyer, R., and Bilmes, J. Submodularity in data subset selection and active learning. In *ICML*, 2015.
- Weiser, M. Programmers use slices when debugging. *Communications of the ACM*, 25(7):446–452, 1982.
- Yeh, C.-K., Kim, J., Yen, I. E.-H., and Ravikumar, P. K. Representer point selection for explaining deep neural networks. In *Advances in Neural Information Processing Systems*, 2018.